

# Research on Timing Synchronization Algorithm for Optical Signal Receiving

Hong-min Wang, Zhong-jie Wang and Ping Xue

*Collage of Automation*

*Harbin University of Science and Technology, Harbin, China, 150000*

*Corresponding Author: Zhong-jie Wang*

*E-mail: 1069730684@qq.com*

## **Abstract**

*In consideration of the characteristics of visible light communication (VLC) and orthogonal frequency division multiplexing (OFDM) signal modulation mode, this paper presents some improvements from two aspects of timing metric function and training sequence structure on the basis of the traditional algorithms. In order to solve the problem of the correlation peak plateau and achieve the symbol accurate positioning, the power of the improved algorithm is normalized on the principle of maximum sliding auto-correlation (SAC). The simulation results show that the improved algorithm can obtain a more excellent timing synchronization performance and a lower symbol error rate (SER) in both the additive white Gaussian noise (AWGN) channel and the multipath frequency selective fading (MFSF) channel. Especially under the environment of a low signal noise ratio (SNR), the improved algorithm has overwhelming advantages over other three traditional algorithms.*

**Keywords:** *Timing Synchronization Algorithm, OFDM, Training Sequence, SAC*

## **1. Introduction**

LED's lighting technology is becoming more mature and widely used, which provides an opportunity for the development of VLC. With white LED as the medium, VLC becomes another new application field of short-range wireless communication for its wide spectrum range, low power consumption, small electromagnetic interference, strong confidentiality and other advantages. Choosing appropriate modulation mode is one of the important ways to improve the transmission rate. Hence, synchronization technology is the key link for the application of the various signal modulation techniques in VLC system [1, 2].

High-speed VLC system is required to overcome multipath fading and improve spectrum utilization. The signal modulation mode of OFDM is used in the transmitter. Due to the strict orthogonality of the subcarriers, the traditional synchronization algorithm is more sensitive to symbol timing deviation (STD) and carrier frequency deviation (CFD). Most of the current researches pursuit high communication speed under the condition of normal SNR while rare ones design algorithm under the condition of low SNR. Aimed to above defects, this paper will improve the system performance from two aspects of timing metric function and training sequence structure.

## **2. Proposed 4th-Order Sigma-Delta Modulator Topology**

The original channel is divided into multiple subchannels by OFDM technology, which converts high-speed serial data streams into low-speed parallel data streams and equilibrates the streams in the frequency domain as a whole. In this way, the computational complexity is sharply reduced. In OFDM signal with subcarriers, the base

band data is modulated on subcarrier. After being transformed by IFFT, the signal at the transmitting terminal is:

$$x(n) = \frac{1}{\sqrt{N}} \sum_{k=0}^{N-1} x_k e^{j2\pi kn/N} \quad (1)$$

Through the static multipath channel of white LED, the signal at the receiving terminal is:

$$y(n) = \sum_{l=0}^{L-1} h(l)x(n - \theta)e^{j2\pi\epsilon n/N} + \omega(n) \quad (2)$$

In the formula,  $L$  is the number SER of light paths;  $h(l)$  is the fading coefficient of certain light path;  $\theta$  is STD normalized by the sampling intervals;  $\epsilon$  is CFD normalized by the subcarrier intervals;  $\omega(n)$  is AWGN.

It is not completely equal that the carrier frequency and the oscillator frequency of the transmitting terminal and the receiving terminal. In order, photocurrent signal produces CFD and sampling clock deviation (SCD) via the down conversion circuit and the analog-to-digital converter (A/D) circuit. The data block can be extracted and demodulated unless the starting position of the signal frame is got by the receiving terminal. The above process is called symbol timing. However, it is difficult to locate the accurate position. Because of this defect, STD arises [3]. Only by estimating and compensating the non-ideal factor of the photoelectric signal, can the receiver operate properly. This serial process is called synchronization. The synchronization of the receiver of indoor VLC system is shown in Figure 1.

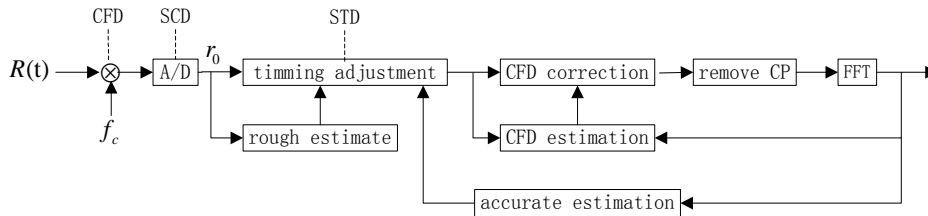


**Figure 1. The Synchronization of the Receiver of Indoor VLC System**

At present, the stability and accuracy of crystal oscillator and A/D module in the wireless communication system are getting better and SCD is getting relatively smaller. Time synchronization is the premise of frequency synchronization. In other words, symbol timing synchronization guarantees carrier frequency synchronization [4]. To sum up, this paper mainly studies the object that the symbol timing synchronization algorithms that influence the performance of VLC communication system.

### 3. Traditional Timing Synchronization Algorithms and Improved Algorithm

Under the environment of VLC, the delay expansion of OFDM signal is defined as inter-symbol interference (ISI). If the guard interval is inserted between adjacent symbols as well as the interval length is longer than the delay expansion of the channel, ISI will be avoided. The last part of the symbol is copied to the head of symbol as a cyclic prefix (CP) to fill in the guard interval. In this way, the delay expansion of CP is directly superimposed on the data, which automatically forms the circuit convolution of OFDM symbol and the channel response, rather than the circuit

reconstruction [5]. In order that the signal in the frequency domain is the circuit convolution of the transmitted data and the channel, FFT receiver window must be located in the range between two guard intervals and after the maximum delay expansion. That is to say, the frame synchronization requires the timing position  $T_0$  to meet the formula below:

$$\tau_{\max} < T_0 < T_{CP} \quad (3)$$

In the formula,  $\tau_{\max}$  is maximum delay expansion in the channel;  $T_{CP}$  is the length of the guard interval. The frame head structure of OFDM symbol added CP is shown in Figure 2:

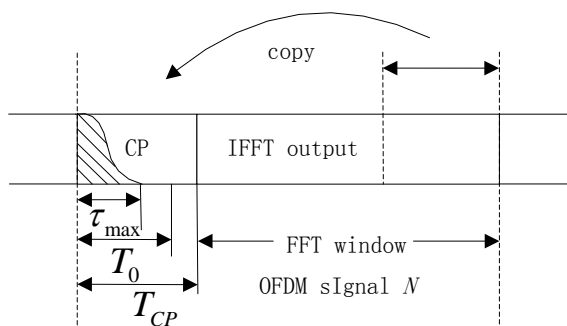


**Figure 2. OFDM Symbol Added CP**

Since CP is the mirror image of the last part of the symbol, the received data are given the treatment of SAC, when the FFT window slides to the starting position of CP. The formula can be got:

$$R_{SAC,n} = \sum_{m=0}^{N_{CP}-1} r_{n+m} r_{n-N+m}^* \quad (4)$$

In the formula,  $r_i$  is the  $i$ th sampling points;  $n$  is the starting point's number of the FFT window;  $m$  is the  $m$ th subcarrier sampling points;  $(\cdot)^*$  means conjugating. At this moment, since the data that will be given SAC at the two ends are completely identical, the correlation reaches a peak value. However, the peak value is affected by noise, interference and other factors, and is not a sharp one, which results in a fuzzy timing position. Especially under the condition of low SNR, the peak will even be drowned in the noise. For the higher reliability and accuracy of timing estimation, some typical algorithms based on training sequence design and the improved one are introduced below.

### 3.1. S&C Algorithm

Schmidt and Cox proposed to set the odd subcarrier to zero and used the even subcarriers to transmit data in the frequency domain. With the method of IFFT, the two halves of training sequence which are transformed to the time domain from the frequency domain are completely identical. At the receiving terminal, the correlation of these two parts can be used in symbol timing estimation and frequency deviation estimation [6]. The frame head structure of S&C algorithm is shown in Figure 3:

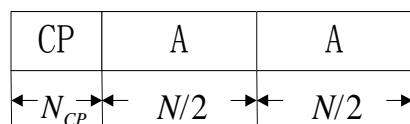


**Figure 3. Training Sequence Designed By S&C**

It is because CP exists in the training sequence that it forms a unique cyclic structure. Above SAC formulas can be referred for the power normalization to achieve the timing synchronization. Timing metric function of S&C algorithm is:

$$M_{S\&C,n} = \frac{|R_{S\&C,n}|^2}{P_{S\&C,n}^2} \quad (5)$$

$$R_{S\&C,n} = \sum_{m=0}^{N/2-1} r_{n+m+N/2} r_{n+m}^* \quad (6)$$

$$P_{S\&C,n} = \sum_{m=0}^{N/2-1} |r_{n+m+N/2}|^2 \quad (7)$$

In these formulas,  $R_{S\&C,n}$  is the correlation value of the two halves of the FFT window;  $P_{S\&C,n}$  is the power of the first half used in the power normalization processing for the correlation value. Through observation, the correlation value can be gained by the iterative method. In more detail, each correlation value can be obtained just by two times of complex multiplication and addition operations.

$$R_{S\&C,n} = R_{S\&C,n-1} + r_{n+N} r_{n+N/2}^* - r_n r_{n+N/2}^* \quad (8)$$

As the front and the rear halves of the training sequence are completely identical, the peak values of SAC can be got when the sliding window is sliding in the CP. Continuous peak values form a phenomenon called “correlation peak plateau” [7].

### 3.2. S&C Optimizational Algorithm

In order to obtain a more accurate timing position and solve the problem of correlation peak plateau, related literatures propose that timing metric function of S&C algorithm is averaged by the sliding window. On the basis of the full use of the original correlation peak plateau, we obtain a steeper curve. Assuming that D is the length of a sliding window, its timing metric function is:

$$\overline{M}_{S\&C/O,n} = \frac{1}{D} \sum_{m=0}^{N_{CP}-1} M_{S\&C/O,n+m} \quad (9)$$

$$M_{S\&C/O,n+m} = \frac{|R_{S\&C/O,n}|^2}{P_{S\&C,n}^2} \quad (10)$$

$$R_{S\&C/O,n} = \frac{1}{2} \sum_{m=0}^{N_{CP}-1} |r_{n+m}|^2 \quad (11)$$

$P_{S\&C,n}$  is the same as above. After careful observation, the diverse terms between two adjacent timing metric functions ( $\overline{M}_{S\&C/O,n}$  and  $\overline{M}_{S\&C/O,n+1}$ ) are  $M_{S\&C/O,n}$  and  $M_{S\&C/O,n+1}$ . By expansion operation, the number of the diverse terms is  $D+1$  [8]. The bigger  $D$  is, the better. When  $D > N_{CP}$ , ISI arises and destroys the orthogonality of the subcarriers. In theory,  $D = N_{CP}$  is the best option. Although the positioning effect is improved, the still insufficient accuracy is not conducive to tracking symbol.

### 3.3. Minn Algorithm

For the sharper correlation peak plateau, Minn proposed that the diverse terms between adjacent timing metric functions can be expanded by changing the frame head structure. Assuming that  $N_{CP} = N/4$  is the length of a sliding window, the frame head structure is shown in Figure 4:

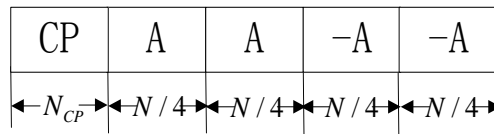


Figure 4. Training Sequence Designed By Minn

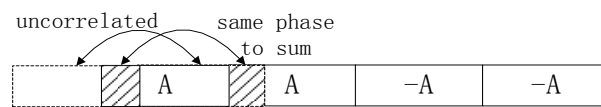
The timing metric function is redefined as:

$$M_{\text{Minn},n} = \frac{|R_{\text{Minn},n}|^2}{P_{\text{Minn},n}^2} \quad (12)$$

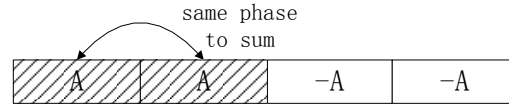
$$R_{\text{Minn},n} = \sum_{k=0}^1 \sum_{m=0}^{N/4-1} r_{n+m+kN/2+N/4} r_{n+m+kN/2}^* \quad (13)$$

$$P_{\text{Minn},n} = \sum_{k=0}^1 \sum_{m=0}^{N/4-1} |r_{n+m+kN/2+N/4}|^2 \quad (14)$$

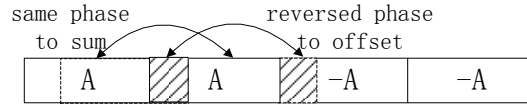
From the above formulas, it can be seen that Minn algorithm is also a cyclic structure of the training sequence given SAC. However, the particularity of its structure can bring some benefits:



a. Sliding window position 1



b. Sliding window position 2



c. Sliding window position 3

**Figure 5. The Sliding Correlation Diagrammatic Sketch of Minn Algorithm**

1. As shown in Figure 5(a), when the sliding window enter the training sequence, the partly same signal in two sliding windows form the same phase superposition after the treatment of correlation ,which makes the slope of the sliding correlation curve values ascend rapidly;

2. As shown in Figure 5(b), when the signals in the sliding windows are completely identical, the correlation value reaches the maximum;

3. As shown in Figure 5(c), the partly same signals in two sliding windows form the reversed phase superposition after the treatment of correlation. The correlation values are offset by each other, which makes the slope of the sliding correlation curve descend rapidly [9, 10].

Theoretical analysis shows that the correlation peak of Minn algorithm is sharper than above ones [11]. However, there are another two side peaks on both sides of dominant peak for the sake of several cyclic structures. The first side peak is the maximum correlation value of third and fourth sequence and the second side peak is the maximum correlation value of fourth sequences and CP. The side peak's energy is about one quarter of that of the dominant peak.

### 3.4. Improved Algorithm

In order to eliminate the interference of the side peak, this paper improves the structure design of the training sequence and the timing metric function. This way maximally expands the difference between two adjacent sampling points. The frame head structure is shown in Figure.6:

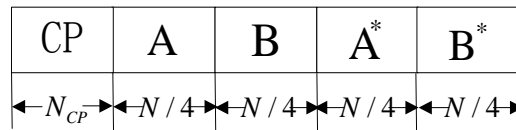


**Figure 6. Training Sequence of Improved Algorithm**

A is made up of pseudo random sequences; B is the mirror image sequence of A. The improved timing metric function is:

$$M_{Imp,n} = \frac{|R_{Imp,n}|^2}{P_{Imp,n}^2} \quad (15)$$

$$R_{Imp,n} = \sum_{k=0}^{N/2-1} r_{n-k-1} r_{n+k} \quad (16)$$

$$P_{Imp,n} = \sum_{m=0}^{N/2-1} |r_{n+k}|^2 \quad (17)$$

In the formula,  $R_{Imp,n}$  is the sum of the product of two sampling points moving in the opposite direction in the continuous length of  $N/2$ . For this kind of structure, when the starting position of the sliding window is in the window  $N/2$ , the data in the front window is the mirror symmetry of the rear window. At this point, the metric function reaches the maximum value. In addition, values in other time domain are about zero. Moreover, the conjugated structure is introduced into the structure of the training sequence, which avoids the conjugated operation in the SAC function and reduces the complexity of the design.

#### 4. Simulation Analysis of Different Algorithms in Two Channels

Simulations are performed respectively in the AWGN channel and MFSF channel. The MFSF channel contains five mutually independent Rayleigh fading channels and the gain of the certain optical path is:

$$h(l) = \frac{\exp(-\tau_i / \tau_m)}{\sqrt{\sum_{k=1}^L \exp(-2\tau_i / \tau_m)}} \quad (18)$$

In the formula,  $\tau_i$  is the time delay of a certain optical path;  $\tau_m$  is the maximum time delay. The simulation parameters in MATLAB are shown in Table 1:

**Table 1. Simulation Parameters**

Simulation term	Set value
FFT sampling points	1024
subcarrier number $N$	1024
the length of CP	256
maximum delay expansion	150
modulation mode	BPSK
carrier frequency	250/MHz
normalized CFD	0.75
simulation times	1000

The simulation results are shown in Figure 7 to 9:

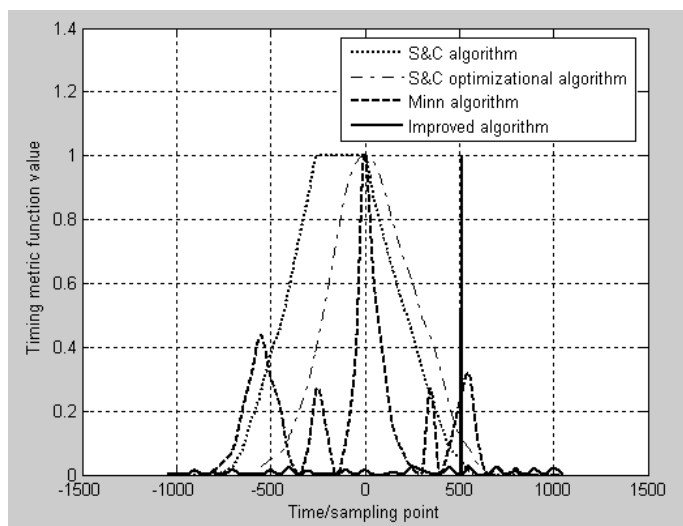


**Figure 7. The Comparison of the Simulation Result of Four Algorithms**

1. The comparison of the timing simulation results of four algorithms are shown in Figure.7: in S&C algorithm, the metric function curve produces correlation peak plateau before the accurate timing position and the width of the plateau is equal to the length of CP; in S&C optimizational algorithm, the metric function based on the original one is averaged which gives rise to phase shifts of ascending curve and descending curve. The metric function curve produces correlation peak fillet in the accurate timing position and the timing effect has been improved; in Minn algorithm, the sharp dominant peak is favorable to capturing the timing position. Meanwhile, there are two side peaks on both sides of dominant peak. The metric function values of side peaks fluctuate around 0.25; in improved algorithm mentioned in this paper, we get a peak value which approximates a pulse when the window slides to  $N/2$ . The peak plateau and the side peaks are eliminated simultaneously and the positioning effect are improved significantly.

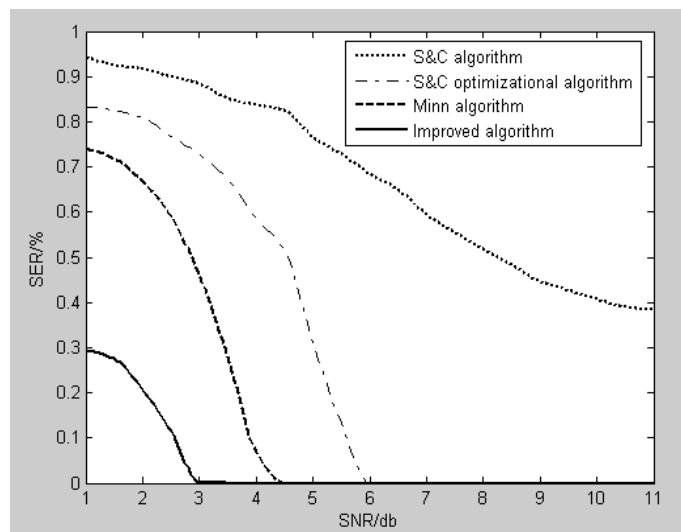


**Figure 8. The Comparison of Algorithms When SER Changes with SNR (AWGN Channel)**

2. In AWGN channel: in S&C algorithm, for the sake of correlation peak plateau, it is possible that the timing position falls at any point within the given range. And uncertainty cannot be significantly improved with the increase of the SNR; in S&C optimizational



algorithm, SNR reaches a specific value and the fillet becomes sharp, then SER reduces to zero; in Minn algorithm, the existence of the side peaks causes the miscalculation of the timing position; in improved algorithm, the timing position is captured more precisely than above three algorithms. When SNR is low, the system still maintains good performance.

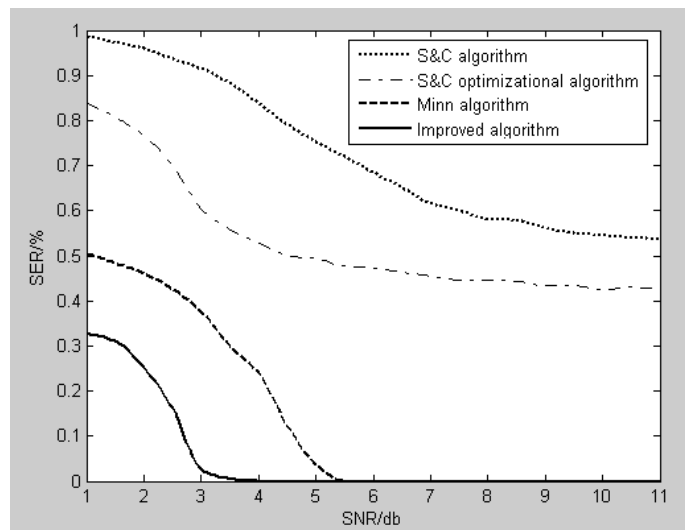


**Figure 9. The Comparison of Algorithms When SER Changes with SNR (MFSF Channel)**

3. In MFSF channel: since S&C algorithm and its optimization are not able to cope with multipath, there are extremums of SER. When  $SNR < 3\text{db}$ , the performance of improved algorithm is more excellent than that of Minn algorithm.

## 5. Conclusion

In VLC system, receiving synchronization algorithm of OFDM signal is directly related to the performance and complexity of the receiver. In this paper's improved algorithm, the conjugate symmetry structure is introduced into the training sequence and the metric function is redesigned. Since the metric function curve has characteristics of the pulse, the phenomenon of correlation peak plateau is eliminated and there is no side peak to interfere with symbol positioning [12]. Whether in AWGN channel or in MFSF channel, both theoretical analyses and simulation results show that improved algorithm can capture the precise timing position and reduce SER in the optical communication. Especially in the conditions of a low SNR, improved algorithm has the overwhelming advantages than other three traditional algorithms. The research result of this paper provides a reliable basis for the next step of the carrier frequency synchronization and the equilibration.

## Acknowledgements

This work is supported by Natural Science Foundation of Heilongjiang Province of China under Grant Nos. F201310 and Special fund for scientific and technological innovation talents of Harbin under Grant Nos. RC2013Q0009007 and Research and development project of Heilongjiang Province under Grant Nos. GC13A412

## References

- [1] F. Yang, L. F. He and C.Y. Pan, "OFDM Principles and Standards: Evolution of Communication Techniques", Beijing, vol. 69, no. 242(2013), Beijing.
- [2] Y. P. Li, "Research on synchronization algorithm for orthogonal frequency division multiplexing system [D]", Harbin: Harbin University of Science & technology, (2012), pp. 45-46.
- [3] C.R. Shu and C.C. Huang, "A differential sliding correlation scheme for symbol timing detection in time domain synchronous OFDM systems", IEEE Vehicular Technology Conference, (2009).
- [4] B. Park, H. Chen, C. Kang and D. Hong, "A novel timing estimation method for OFDM systems", IEEE Communications Letters, (2003).
- [5] S. Ye, "Research of Indoor Visible Light Communication System Based on OFDM", Huazhong University of Science & technology, (2013).
- [6] Q. Chen, C. Y. Fu, Y. Hong and W. Deng, "Key Technologies of Improving System Performance of Indoor Visible Light Communication", Automation & Information Engineering, (2010), pp. 4-7.
- [7] J. Zhao, "Study on Visible Light Communication System Based on White LED Array Source", Guangzhou, Jinan University, (2009).
- [8] H. Zhang, Z. X. Song, D. Y. Liu, X. B. Zhou and L. H. Yin, "Research on Indoor Visible Light Communication System Based on Adaptive OFDM", Journal of Changchun University of Science and Technology(Natural Science Edition), (2010), pp. 70-73.
- [9] X. Li, "Research on adaptive resource allocation for OFDM system [D]", Harbin: Harbin University of Science & technology, vol. 13, (2015).
- [10] R P. Gilliard, M. D. Vincentia and A Halide, "Operation of the LiFi light emitting plasma in resonant cavity", IEEE Transactions on Plasma Science, pp. 1026-1033, (2011).
- [11] International Conference on. IEEE, (2013), pp. 875-878.
- [12] R. Gilliard, "The LiFi® lamp high efficiency high brightness light emitting plasma with long life and excellent color quality", //Plasma Science, (2010).